Natural Hazards (2019) 97:841–860
https://doi.org/10.1007/s11069-019-03678-1

ORIGINAL PAPER

Damage demands evaluation of reinforced concrete frame structure subjected to near-fault seismic sequences

Fujian Yang[1] · Guoxin Wang[1] · Yang Ding[1]

Received: 9 August 2017 / Accepted: 17 July 2019 / Published online: 24 July 2019

Abstract
The design earthquake is usually specified as a single event in most of modern seismic codes. However, one earthquake is often followed by a series of aftershocks called seismic sequence. Such cases are quite common, especially in near-fault regions, which could cause additional accumulated damage to structures. In this paper, a new methodology for evaluating the effect of near-fault seismic sequences on the accumulated damage of reinforced concrete (RC) frame structure is proposed, in which different initial damage levels (i.e., postmainshock global damage index) of structure after the mainshock are considered. Meanwhile, a quantitative description of the damage demands and the relative intensity index between mainshock and aftershock are provided. For this purpose, the nonlinear dynamic response of an eight-story RC frame structure subjected to single earthquake and seismic sequence is compared in terms of structural performance indices (collapse capacity, story damage demands, postmainshock damage level and normalized hysteretic energy) and relative intensity index. The results indicated that seismic sequences lead to reduced collapse capacity of postmainshock-damaged structures. Moreover, the near-fault pulse-like aftershock records would induce larger structural story damage demands than ordinary (i.e., non-pulse-like) aftershock records. Furthermore, the relative intensity index proposed in this paper has significant effects on the structural story damage demands, incremental dynamic analysis curves of aftershock and normalized hysteretic energy.

Keywords Seismic sequence · Near-fault ground motion · Story damage demand · Damage index · Relative intensity index · Reinforced concrete frame structure

1 Introduction

Massive historical seismic damages have shown that earthquake events are usually not single events, often followed by a series of shocks in a certain time, forming the foreshock, mainshock and aftershock sequences. A stronger mainshock always accompanies more and larger foreshocks or aftershocks; some of these seismic sequences can last for several years

✉ Fujian Yang
fjyang@outlook.com

[1] State Key Laboratory of Coastal and Offshore Engineering, Dalian University of Technology, Dalian 116024, China

and even longer. For example, the 2016 Kumamoto (Japan) seismic sequence contains a series of strong earthquakes, including a mainshock with a magnitude of M_w 7.0 which struck on April 16, 2016, beneath Kumamoto City in Kyushu region, Japan, and a foreshock with a magnitude of M_w 6.2 on April 14, 2016. Besides, the Wenchuan earthquake (M_w 8.0, May 12, 2008) occurred in Sichuan province of China had 6, 42,719 aftershocks from May 12 to November, in which 8 aftershocks had magnitudes larger than 6.0. Strong aftershocks are usually unpredictable like mainshock, could aggravate damage and even induce collapse of the postmainshock-damaged structures. In addition, most of the modern seismic codes only take into account single earthquake without considering the influence of the entire seismic sequence. Consequently, it is of great importance and urgency to investigate the effects of aftershock on the dynamic response and accumulated damage demands of postmainshock-damaged structures.

Recently, there has been increasing interest in the field of civil engineering for evaluating the influence of mainshock–aftershock sequences or repeated earthquakes on structures. Most of these studies employed single degree of freedom (SDOF) systems to analyze the dynamic response of structure subjected to seismic sequences. The SDOF system, having the advantage of sample structural form and fast calculation, is widely applied in evaluating the effect of seismic sequences on structures. These investigations focused on the inelastic response analysis, such as inelastic displacement ratio (Durucan and Durucan 2016; Hatzigeorgiou and Beskos 2009), ductility demand (Goda 2012; Goda and Taylor 2012; Hatzigeorgiou 2010b; Rinaldin et al. 2017), behavior factor (Amadio et al. 2003; Fragiacomo et al. 2004; Hatzigeorgiou 2010a), strength reduction factor (Zhai et al. 2015; Zhang et al. 2017) and damage spectra (Moustafa and Takewaki 2011; Zhai et al. 2013) under seismic sequences. Hosseinpour and Abdelnaby (2017a) pointed out that SDOF system introduced a large number of assumptions, neglecting localized behavior, force redistribution and the effect of higher modes. Obviously, multi-degree of freedom (MDOF) systems can better reflect the dynamic behavior of real structures than SDOF system. Therefore, in recent years, more and more researchers have focused on the effect of seismic sequences on MDOF systems. For example, Hatzigeorgiou and Liolios (2010) investigated the inelastic response of eight RC frames comprising both regular and vertically irregular structures when subjected to five as-recorded seismic sequences and forty artificial seismic sequences. They estimated the ductility demands under seismic sequences by using an empirical expression with an appropriate combination of the corresponding ductility demands under single earthquake. Ruiz-García and Negrete-Manriquez (2011) studied the drift demands of existing steel frames with a different number of stories subjected to as-recorded near-fault and far-field seismic sequences. They found that the frequency contents of the mainshock and aftershock are quite different. They indicated that the peak and residual drift demands have not significantly increased under as-recorded seismic sequences, while the artificial seismic sequences could overestimate median peak and residual drift demands. Ruiz-García et al. (2014) also evaluated the nonlinear response of four RC buildings with a different number of stories under seismic sequences. Results showed that the relationship between the period of mainshock-damaged structure and predominant period of the aftershock has a significant impact on the structural response. Abdelnaby and Elnashai (2014) investigated the degrading behavior of RC frame systems subjected to multiple earthquakes. They used fiber-based finite element models in which the steel and concrete have different degrading features to evaluate the nonlinear response of these models. The results indicated that multiple earthquakes have a significant effect on the structural nonlinear response. Hosseinpour and Abdelnaby (2017b) studied the fragility curves for RC frames under as-recorded multiple earthquake. They observed that different parameters,

including damage from previous event, vertical earthquake component, earthquake region, number of stories and earthquake intensity, significantly affect fragility curves. Faisal et al. (2013) investigated ductility demands of three-dimensional inelastic concrete frames under repeated earthquakes. They observed a significant increase in the ductility demands when considering multiple earthquakes. Hatzivassiliou and Hatzigeorgiou (2015) studied the effects of seismic sequences on two regular and two irregular buildings. Results showed that seismic sequences significantly increase seismic demands and the siting configurations affect structural ductility demands. Wang et al. (2017) evaluated the damage of mainshock-damaged concrete gravity dams under as-recorded seismic sequences. The results showed that the aftershocks significantly increase the damage demands of the dam which is already damaged under single seismic event and has not been repaired. They also revealed that the repeated seismic sequences tend to underestimate the level of damage demands.

It should be noted that although some studies have evaluated the structural behavior subjected to seismic sequence, there are still some limitations. Most of the aforementioned studies focused on the effect of seismic sequences on the seismic demands of civil structures (RC frame, steel frame, gravity dams, etc.). To the best of the authors' knowledge, few studies in the literature took the damage demands as the structural accumulated damage measure to investigate the effect of seismic sequences on building structure, in which most studies aimed at assessing the damage of the component section or the entire structure (Hatzigeorgiou and Liolios 2010; Zhai et al. 2014). However, due to panel mechanisms, the collapse of structures usually starts at a certain floor and gradually extends to the overall structure. Therefore, the story damage demands should be developed as a quantitative measure to evaluate the accumulated damage of structures. In addition, most seismic codes assume far-field earthquake records to describe the seismic actions, while the earthquakes recorded in the near-fault region presented as a pulse waveform in the velocity time history due to forward-directivity effect, which are quite different from far-fault ground motions. Pulse-like ground motions can induce significant seismic demands on structures in the near-fault region (Kalkan and Kunnath 2006). Consequently, the effect of near-fault seismic sequences on structures is worth to further study. Recently, it is of particularly interest to further investigate the effect of the frequency characteristics of the aftershock on the structural dynamic response (Ruiz-García and Negrete-Manriquez 2011; Ruiz-García 2012; Ruiz-García et al. 2014, etc.). From results of these studies, it is concluded that the frequency characteristics of the earthquake records have a significant effect on the structural dynamic response. However, these studies only focused on the effect of predominant period of mainshock–aftershock on the nonlinear response of structures. Few investigations involve ground motion parameters related to characteristics in frequency domain, such as *V/A* (i.e., ratio of the peak ground velocity (PGV) to peak ground acceleration (PGA), units in seconds) (Tso et al. 1992). In addition, in near-fault region, ground motions with directivity effects tend to bring higher *V/A* ratio, which dramatically influences their response characteristics (Malhotra 1999). Therefore, it is very interesting to explore the effect of the *V/A* ratio of mainshock and aftershock in the near-fault region on the structural accumulated damage.

The objective of this paper is to evaluate the effect of near-fault seismic sequences on the damage demands of RC frame structure with different initial damage levels after the mainshock action. For this purpose, a story damage index has been developed to assess the structural accumulated damage caused by aftershocks. In addition, in order to evaluate the influence of the frequency characteristics of aftershock on the damage demands in depth, the relative intensity index between mainshock and aftershock is provided. Finally, the nonlinear response analysis of frame structure is performed under constructed seismic

sequences consisting of 18 near-fault pulse-like and 9 near-fault ordinary recorded earthquakes. All these studies were carried out using an eight-story reinforced concrete (RC) frame structure modeled in OpenSees (Mazzoni et al. 2014) software. Specific goals of the research reported in this paper are: (a) to investigate the effect of aftershock on the collapse capacity of mainshock-damaged structure; (b) to identify the different story damage demands of mainshock-damaged structure under pulse-like aftershocks and ordinary aftershocks in the near-fault region; (c) to investigate the effect of the relative intensity index proposed by this study and the different initial damage levels on the structural story damage demands, the aftershock IDA curves and the normalized hysteretic energy.

2 Methodology

2.1 Definition and classification of damage level

In order to quantitatively evaluate the accumulated damage of structures under seismic sequence, a reasonable structural damage index is necessary. For this purpose, based on the well-known Park–Ang model (Park et al. 1985), the modified Park–Ang damage index (DI) proposed by Kunnath et al. (1992) is employed in the present study to assess the damage of structures which considers both the maximum deformation and the hysteretic energy of structural members. The modified Park–Ang damage index is defined as:

$$\mathrm{DI} = \frac{\theta_\mathrm{m} - \theta_\mathrm{r}}{\theta_\mathrm{u} - \theta_\mathrm{r}} + \beta \frac{E_\mathrm{H}}{M_\mathrm{y}\theta_\mathrm{u}} \tag{1}$$

where θ_m is the maximum curvature of member section under earthquake ground motions, θ_r is the recoverable curvature when the section reaches the maximum deformation, θ_u is the corresponding ultimate curvature capacity of section under monotonic loading and M_y is the yield moment capacity. E_H is the hysteric energy dissipation of member under earthquake ground motion, and β is a model constant parameter to scale the effect of hysteric energy dissipation on the final damage of structure. The experimental values of β reported in Ph.D. thesis (Park 1984) ranged between about -0.3 and $+1.2$, with a median of about 0.15 (Cosenza and Manfredi 2000; Zhang et al. 2017). This damage index can also be extended to the story and overall levels (i.e., story damage index, $\mathrm{DI_s}$, and global damage index, DI) of a structure; by combining the component-based damage indices with a self-weight, the story or overall levels damage index is defined as:

$$\mathrm{DI} = \frac{\sum_{i=1}^{N} \omega_i \mathrm{DI}_x^2}{\sum_{i=1}^{N} \omega_i \mathrm{DI}_x} \tag{2}$$

where DI indicates the story damage index or global damage index of structure, when DI is the story damage index, DI_x means the damage index of member; when DI is the global damage index, DI_x means the story damage index ($\mathrm{DI_s}$). N is the number of the members on a certain floor or the number of total story, and ω_i is the importance factor for the member or story.

It is recommended that the members of story should be allocated according to importance when quantifying damage (Bertero et al. 1974). A philosophy of strong column weak beam is recommended in seismic design of structure. Since a collapse at lower story levels

likely causes the collapse of the entire structure, the lower story levels may be considered of greater structural importance than upper levels. On the other hand, the lower structure could probably remain undamaged when an upper story level collapses. Therefore, the method proposed herein uses the total tributary gravity load as the criterion for assigning importance factors for a member; the important factor ω_i is calculated according to Eq. (3):

$$\omega_i = \frac{GL_i}{\sum_{i=1}^{N} GL_i} \tag{3}$$

where GL_i indicate that total tributary gravity load of ith structural member; N is the number of all structural members.

In order to determine the interrelation between the damage level (e.g., minor damage, moderate damage, severe damage, near collapse and collapse) and the damage index resulting from modified Park–Ang model, the detailed classification of damage levels suggested by Zhang et al. (2017) is adopted to describe the structural damage states. Table 1 summarizes the ranges of damage indices associated with a certain damage level. Accordingly, four damage indices $DI_o = 0.2, 0.4, 0.6, 0.8$ (representing minor damage, moderate damage, severe damage and near collapse, respectively) are selected as the original damage states of mainshock-damaged structure in this study.

2.2 The aftershock damage assessment procedure

In this study, an assessment procedure for evaluating the accumulated damage under aftershocks is presented, which takes into account different initial damage levels of the building model after the mainshock excitation. Particularly, this procedure can be used to evaluate the aftershock collapse capacity and accumulated damage of building model against aftershock. The steps of the assessment procedure are summarized as follows:

(1) Establish a suitable numerical analytical model of a given building in its undamaged condition.
(2) Select a suitable set of as-recorded near-fault seismic records, according to the randomized approach introduced by Hatzigeorgiou and Beskos (2009) to construct near-fault mainshock–aftershock seismic sequence.
(3) For a given mainshock–aftershock seismic sequence, select different initial damage levels (e.g., the global damage index or maximum story damage index) after mainshock excitation (i.e., $DI_o = 0.2, 0.4, 0.6$ and 0.8).

Table 1 Damage index ranges for different damage levels (from Zhang et al. 2017)

Damage level	Damage index range
Negligible	$0 < DI < 0.1$
Minor	$0.1 < DI < 0.2$
Moderate	$0.2 < DI < 0.5$
Severe	$0.5 < DI < 0.8$
Near collapse	$0.8 < DI < 1.0$
Collapse	$1.0 < DI$

(4) Execute the incremental dynamic analysis (IDA) (Vamvatsikos and Cornell 2002) for the undamaged building model until the undamaged building model reaches the selected target postmainshock damage states under the scaled mainshock ground motion.
(5) Perform damage analysis of the leaned building (i.e., in its postmainshock state) under the corresponding aftershock ground motion.

As a demonstration to construct seismic sequence procedure (i.e., steps 1–4), the ground motion record of the 1994 Northridge earthquake at the Jensen Filter Plant Administrative station (i.e., JFP station) is selected. Firstly, the IDA is carried out for the mainshock ground motion until the original (i.e., undamaged) structural model reaches four target DI_o values. Accordingly, the PGA values of mainshocks (i.e., PGA_{ms}) corresponding to the four DI_o values are obtained. Then, the aftershock in constructed near-fault seismic sequence will be scaled according to the ratio between PGA_{as} and PGA_{ms} (i.e., $PGA_{as}/PGA_{ms}=0.8526$). Figure 1 shows the IDA curve of the 1994 Northridge earthquake recorded at the JFP station, in which the $PGA_{ms}=0.183$ g, 0.230 g, 0.266 g, 0.285 g corresponding to $DI_o=0.2$, 0.4, 0.6, 0.8, respectively.

3 Structural model and seismic sequences

3.1 Building frame model

In order to illustrate the proposed aftershock assessment procedure, one regular eight-story three-bay RC frame structure, located in a high-seismicity region of China, is considered in this study. This frame structure considers both gravity and seismic loads with the design PGA of 0.2 g, the design fortification intensity VIII, the first design earthquake group and II category site condition (i.e., mediate-dense sands and hard rock), which is designed following the current Chinese codes (GB50010-2010; GB50011-2010). Figure 2 illustrates the plan view, elevation, rebars and shape of the sections of the analyzed frame. The first story has a height of 4.5 m, while the remaining stories have 3.6 m. It should be mentioned

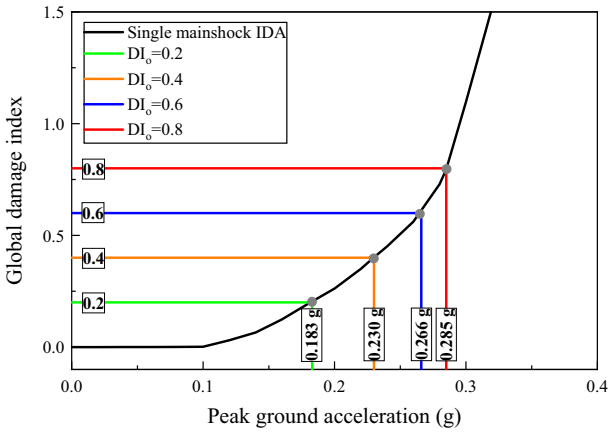

Fig. 1 IDA curve of the building model under single mainshock action (i.e., recorded at JFP station, 1994 Northridge earthquake)

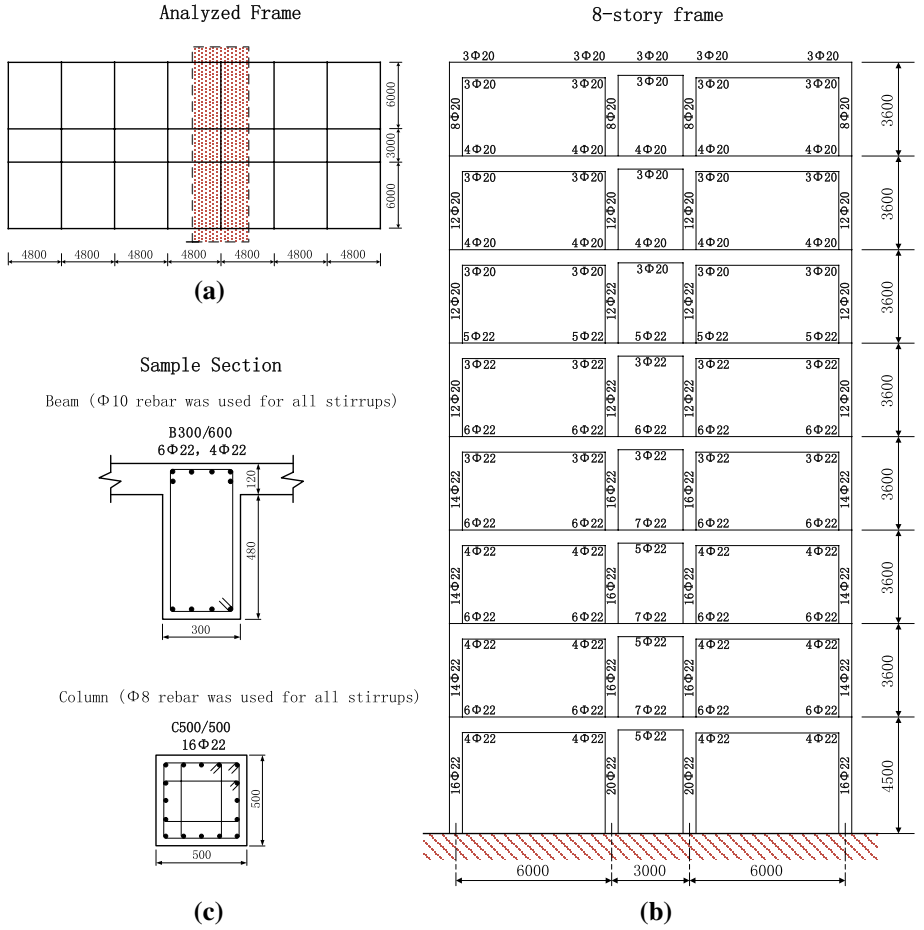

Fig. 2 **a** Plan view, **b** elevation, **c** rebars and shape of sample sections of eight-story frame building (units in mm)

that this structure has uniform distributions of mass, stiffness and strength in horizontal and vertical directions. The sectional dimensions are summarized in Table 2.

The detailed design of the longitudinal and transverse reinforcement of beams and columns is carried out according to the principles of capacity design. The compressive

Table 2 The sectional dimensions of this eight-story frame structure

Story	External column Size (mm)	Interior column Size (mm)	External beam Size (mm)	Interior beam Size (mm)
1–3 floors	550×550	550×550	300×600	250×550
4–6 floors	500×500	500×500		
7–8 floors	450×450	450×450		

strength of concrete is 20.1 MPa (i.e., concrete grade C30), and the yield strength for the steel is 400 MPa. The thickness of concrete protective layer and slab is 30 mm and 120 mm, respectively. According to the building code (GB50010-2010), the dead load (DL) and live load (LL) are considered as 5.0 kN/m^2 and 2.0 kN/m^2 on typical floors, respectively. On the roof, 6.5 kN/m^2 and 0.5 kN/m^2 are taken by DL and LL, respectively. The first mode natural period of the structure is 1.372 s.

The structural analysis is performed using the nonlinear dynamic analysis computer program OpenSees (Mazzoni et al. 2014), which considers both the geometric and material nonlinear behaviors of structural models. Only interior frame (See Fig. 2a) of the building is selected and modeled as a two-dimensional (2D) centerline model due to its symmetry in the building's horizontal plane. It is assumed that the frame model is fixed on the rigid ground which implies that soil–structure interaction is neglected. The fiber-based finite element model is selected to model the nonlinear beam columns and the P-delta effect (i.e., large displacement analysis). This element provides a good balance between accuracy and computational cost (Fragiadakis and Papadrakakis 2008). The modified Kent–Park model (Kent and Park 1971, Concrete02 material in OpenSees) is adopted for the simulation of the concrete constitutive behaviors, considering that it allows for accurate prediction of the structural demand for flexure dominated RC members despite its relatively simple formulation. To consider the constraint of stirrups on concrete in the core zone, the Mander method (Mander et al. 1988) was employed. The inelastic behavior of steel reinforcements is simulated with the model proposed by Menegotto and Pinto (1973) (Steel02 in OpenSees). These constitutive models allow for good consideration of stiffness and strength degradation. The stress–strain relation of concrete and steel reinforcements is shown in Fig. 3. More details on modeling can be found in Mazzoni et al. (2014).

3.2 Mainshock–aftershock sequences

The sequence-type ground motion records are usually composed of one main mainshock (i.e., the event with the largest earthquake magnitude) and multiple aftershocks, which can be classified as single earthquake (mainshock only), two earthquakes sequence (mainshock plus one aftershock), three earthquakes sequence (mainshock plus two aftershocks), etc.

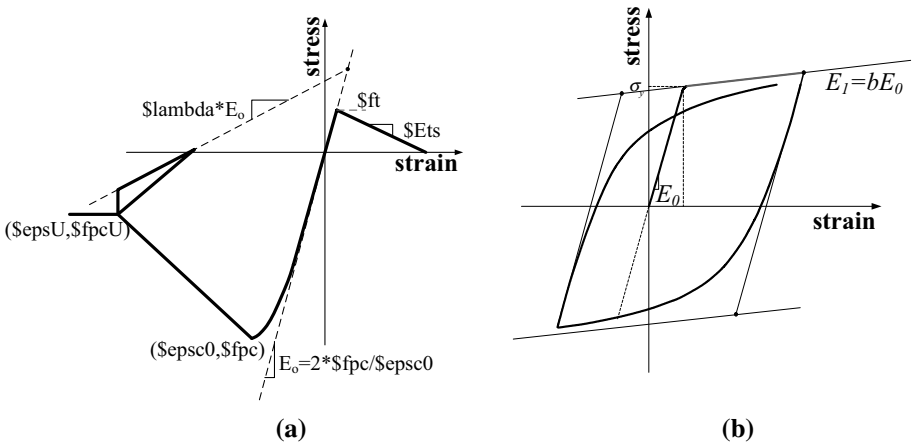

Fig. 3 Materials constitutive model of **a** concrete and **b** steel reinforcement

Scenario of two earthquakes sequence has been commonly employed in previous studies (e.g., Goda and Taylor 2012; Zhai et al. 2014; Ruiz-García and Aguilar 2015; Zhang et al. 2017). Their results indicated that the valuable information about the influence of aftershock can be obtained from the two earthquakes sequence. Therefore, one mainshock plus one aftershock sequence-type ground motion is specified in this study.

In order to describe the important features of actual seismic sequences and obtain valuable conclusions about the effects of aftershocks, constructed seismic sequences which can consider different frequency characteristics of mainshock–aftershock sequences are adopted as the input motions for structural dynamic analysis in this study. To the best of the authors' knowledge, two approaches for constructing seismic sequences are commonly used in the literature. The first approach is repeated approach which repeats the identical mainshock record, with scaled or identical amplitude, as an aftershock time history. It must be noticed that this approach assumes that the frequency content and duration of mainshock and aftershock are the same, which is obviously inaccurate. Recent investigations have found that the repeated approach overestimates the effect of aftershock on the structural response (Ruiz-García and Negrete-Manriquez 2011; Ruiz-García 2012). The second one is the randomized approach introduced by Hatzigeorgiou and Beskos (2009), in which proper scaling factor was proposed for computing the amplitude of aftershock ground motions. The seismic sequence generated using this approach consists of two randomly selected earthquake records, according to a relative strength relation between the two successive records (i.e., mainshock–aftershock). The randomized approach has been commonly used in the literature (e.g., Hatzigeorgiou and Beskos 2009; Hatzigeorgiou 2010a, b; Faisal et al. 2013; Ruiz-García et al. 2014; Morfidis and Kostinakis 2017). Therefore, the randomized approach proposed by Hatzigeorgiou and Beskos (2009) is employed to generate mainshock–aftershock sequence in this study.

Moreover, this study focuses on the effect of aftershock on accumulated damage of RC frame structure located in the near-fault region, where pulse-like ground motions are often observed. For this purpose, two types of two seismic sequences in the near-fault region are identified and selected as follows: (1) near-fault pulse-like + near-fault pulse-like (NP–NP); (2) near-fault pulse-like + near-fault ordinary (NP–NO).

In order to construct seismic sequences, an adequate number of real single earthquake records should be selected. In this paper, a dataset consisting of 18 horizontal near-fault pulse-like seismic records and 9 horizontal near-fault ordinary seismic records is selected from the PEER (Pacific Earthquake Engineering Research Center) strong motion database according to the following criteria: (1) All records should be recorded in the near-fault region (i.e., the distance to the fault is within 15 km, as the Uniform Building Code (UBC 1997) suggests); (2) available information about the soil condition, which corresponds to NEHRP soil types B, C and D; (3) moment magnitude, M_w, equal to or greater than 6.0; (3) the PGA values of all ground motion records should exceed 0.1 g; (4) the *V*/*A* ratio is between 0.04 s and 0.31 s. The characteristics of the selected ground motions are shown in Table 3. Figure 4 illustrates spectral acceleration of the 31 earthquake records with 5% damping ratio used in the present study. To consider different frequency characteristics between mainshock and aftershock, the *V*/*A* ratio is selected as ground motion intensity measure. Firstly, four records in Table 3 with *V*/*A* ratio = 0.20 s, 0.25 s, 0.26 s and 0.28 s were employed as mainshock ground motions (marked as **M1**, **M2**, **M3** and **M4** in Table 3) which represent a different intensity of mainshock. Then, the same PGA scaling factors are applied to each of the

Table 3 List of near-fault ground motions ($R^a < 15$ km) employed to derive the artificial seismic sequences considered in this investigation

No.	Year	Event	M_w	Station	Comp.	R^a (km)	PGA (g)	PGV (cm/s^2)	V/A^b (s)
Near-fault pulse-like records									
M1	1994	Northridge	6.7	Jensen Filter Plant A.B.	022	5.4	0.41	111.47	0.28
M2	1979	Imperial Valley	6.5	El Centro Array #5	230	4.0	0.38	96.90	0.26
M3	1979	Imperial Valley	6.5	El Centro Array #7	230	0.6	0.47	113.14	0.25
M4	1989	Loma Prieta	6.9	Saratoga—W Valley Coll.	270	9.3	0.33	64.91	0.20
1	1999	Chi–Chi	7.6	CHY101	EW	9.9	0.34	65.00	0.20
2	1999	Chi–Chi	7.6	TCU102	EW	1.5	0.30	91.72	0.31
3	1994	Northridge	6.7	Newhall—W Pico Canyon Rd.	046	5.5	0.42	118.18	0.29
4	1994	Northridge	6.7	Rinaldi Receiving Sta	228	6.5	0.87	148.00	0.17
5	1994	Northridge	6.7	Sylmar—Olive View Med FF	360	5.3	0.84	129.37	0.16
6	1979	Imperial Valley	6.5	El Centro Array #10	050	8.6	0.17	50.69	0.30
7	1979	Imperial Valley	6.5	El Centro Array #4	230	7.1	0.37	80.41	0.22
8	1979	Imperial Valley	6.5	El Centro Array #6	230	1.4	0.45	113.55	0.26
9	1979	Imperial Valley	6.5	El Centro Differential Array	270	5.1	0.35	75.58	0.22
10	1995	Kobe	6.9	Kobe University	000	0.9	0.28	55.30	0.20
11	1999	Kocaeli	7.5	Izmit	090	7.2	0.23	38.29	0.17
12	1999	Kocaeli	7.5	Yarimca	060	4.8	0.23	69.72	0.31
13	1989	Loma Prieta	6.9	Gilroy—Historic Bldg.	160	11.0	0.29	43.39	0.16
14	1989	Loma Prieta	6.9	Gilroy Array #3	090	12.8	0.37	45.43	0.13
Near-fault ordinary records									
1	1976	Gazli	6.8	Karakyr	090	5.5	0.86	67.65	0.08
2	1999	Chi–Chi	7.6	TCU084	NS	11.5	0.43	48.09	0.10
3	1979	Imperial Valley	6.5	Bonds Corner	230	2.7	0.78	44.94	0.06
4	1979	Imperial Valley	6.5	Chihuahua	012	7.3	0.27	24.80	0.09
5	1985	Nahanni	6.8	Site 1	010	9.6	1.11	43.93	0.04
6	1989	Loma Prieta	6.9	BRAN	090	10.7	0.50	44.49	0.09
7	1989	Loma Prieta	6.9	Corralitos	000	3.9	0.64	55.97	0.09
8	1994	Northridge	6.7	LA—Sepulveda VA Hospital	360	8.4	0.93	76.27	0.08
9	1994	Northridge	6.7	Northridge—17645 Saticoy St	090	12.1	0.34	31.44	0.09

[a]Closest distance to rupture plane

[b]The ratio of peak ground velocity (PGV) and peak ground acceleration (PGA)

aftershock records: $PGA_{ms}/PGA_{as} = 1.000:0.8526$, according to the approach of Hatzigeorgiou and Beskos (2009) and Hatzigeorgiou (2010a). Finally, the selected mainshock and aftershock time histories are connected considering a gap of 50 s between the two successive earthquake records. This interval is sufficient for the structure to reach a steady state under damping. Figure 5 shows acceleration time histories of the successive mainshock–aftershock artificial seismic sequence. In addition, the frame structure will reach four target damage states (i.e., $DI_o = 0.2$, 0.4, 0.6 and 0.8) and the corresponding

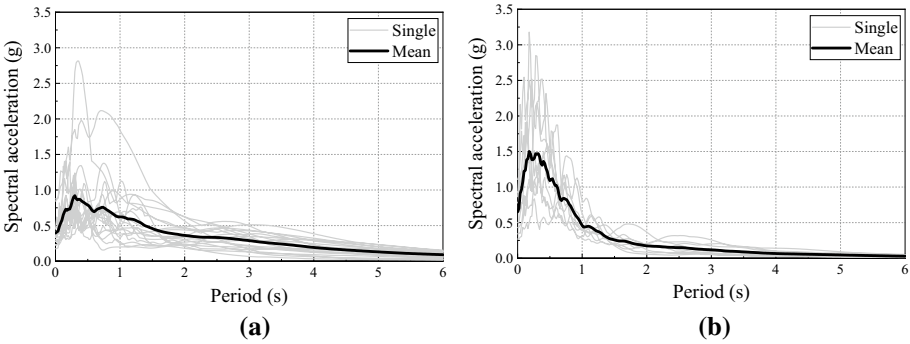

Fig. 4 Elastic acceleration response spectra of **a** near-fault pulse-like and **b** ordinary ground motions with 5% damping ratio

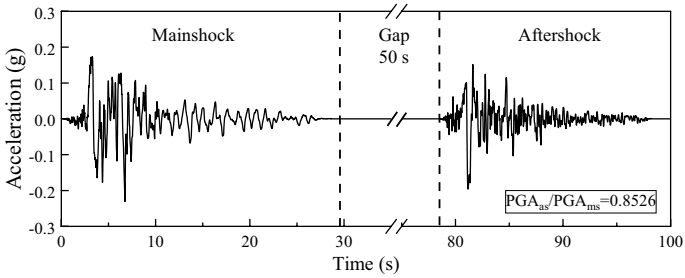

Fig. 5 Acceleration time histories of the constructed mainshock–aftershock sequence

PGA values of four mainshocks are obtained through IDA. Therefore, a total number of 416 artificial sequences were generated randomly for all DI_o.

4 Aftershock collapse assessment under seismic sequence

In this section, the collapse capacity of the structure under seismic sequence is evaluated. Initially, only the mainshock IDA is carried out until the global damage index of building model reaches collapse limitation (i.e., DI = 1.0). Then, the mainshock PGA corresponding to DI = 1.0 is obtained, which is taken as the mainshock collapse capacity (i.e., $PGA_{c,\,ms}$). Subsequently, the amplitude of the mainshock record is scaled so that the undamaged building reaches four different target DI_o values after performing nonlinear dynamic analysis. Then, the aftershock IDA is conducted and the aftershock collapse capacities (i.e., $PGA_{c,\,as}$) of different DI_o values are computed. Figure 6 shows the aftershock IDA curves with different DI_o values and the mainshock IDA curves with two constructed seismic sequences. It is obvious that the $PGA_{c,\,as}$ decreases with respect to the $PGA_{c,\,ms}$ regardless of target DI_o. For example, the $PGA_{c,\,as}$ decreases from about 0.42–0.32 g for target $DI_o = 0.6$ in Fig. 6a. Besides, it can be clearly seen that the $PGA_{c,\,as}$ depends on the level of DI_o and decreases with the increase in DI_o. For example, $PGA_{c,\,as}$ for a DI_o of 0.2 (green point) reduces from about 0.38 g to 0.30 g for a DI_o of 0.8 (red point). Similar trend can be observed in Fig. 6b.

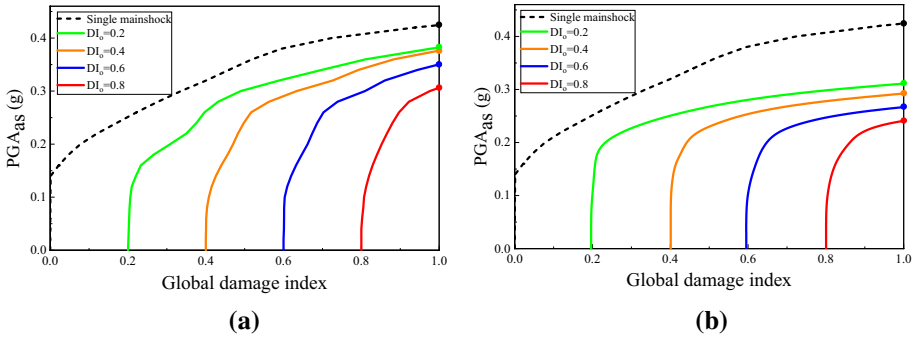

Fig. 6 Mainshock and aftershock IDA curves with different DI_o values to obtain the eight-story structural model collapse capacity under **M3** mainshock (i.e., El Centro Array #7 comp. 270) and seismic sequences. **a** Aftershock recorded at Kobe University, **b** aftershock recorded at El Centro Array #6

5 Comparison of story damage demands under pulse-like and ordinary aftershock

In order to quantitatively study the effect of seismic sequences on the story damage demands, the story damage index (DI_s) presented in Eq. (2) is used, in which the structural story damage index is defined as the damage value of a story along the elevation and obtained by weighting the damage value of the beam and column members on this story. It is worth noting that at the member level, the maximum of the two joint indices is used to represent the component damage index.

Ground motions close to a ruptured fault resulting from forward-directivity effect are significantly different from those observed far away from the seismic source. In order to investigate the influence of near-fault seismic sequences on the RC frame structure, especially the effect of pulse-like (NP) and ordinary (NO) aftershock records on the story damage demands of the structure, a series of nonlinear dynamic analyses are performed using NP–NP and NP–NO constructed seismic sequences. Figure 7 shows the distribution of average story damage under near-fault pulse-like and ordinary aftershock after

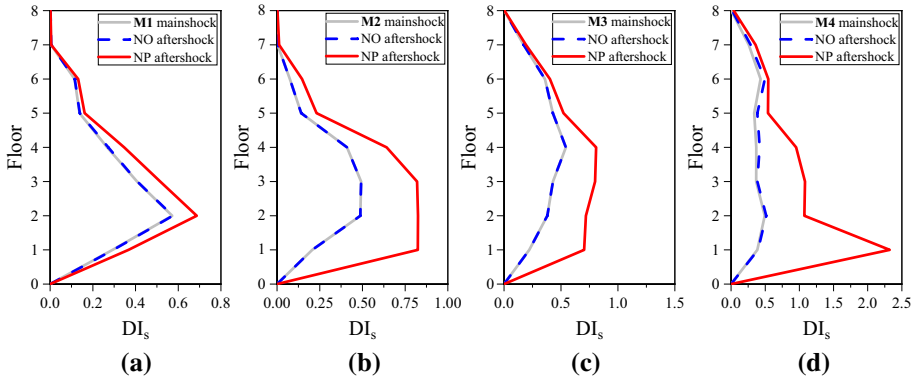

Fig. 7 Height-wise distribution of average story damage index computed from near-fault pulse-like and non-pulse aftershock. **a M1** mainshock, **b M2** mainshock, **c M3** mainshock, **d M4** mainshock

four different intensity mainshocks action (i.e., **M1**, **M2**, **M3** and **M4**) when $DI_o = 0.4$. As expected, the NP aftershocks induce larger story damage values than the NO aftershocks which tends to concentrate in the ground story since it was anticipated that the frame could develop a ground soft story mechanism. Moreover, from the figures, it is observed that the NP–NO seismic sequences do not increase the level of story damage demands compared with the single mainshocks and NP–NP seismic sequence. Although the two types of aftershocks have the same PGA, the results are quite different. The situation illustrates that it is insufficient only to take the PGA as the damage potential parameter for the mainshock and aftershock. On the other hand, the fundamental natural period of the structure will increase after the mainshock action, and pulse-like records have a larger long period component than the ordinary records in the spectral acceleration. Therefore, the frequency characteristics of aftershocks have a significant influence on the seismic performance of structures.

6 Effect of parameter κ

6.1 Definition of the relative intensity index

For earthquakes, the *V*/*A* ratio, which is the ratio between PGV and PGA, is taken as the seismic intensity indicator, because it can reflect the frequency characteristics of ground motions (Tso et al. 1992). In this paper, the relative intensity index, κ, is defined as the *V*/*A* ratio of the aftershock to the mainshock:

$$\kappa = \frac{(V/A)_{\mathrm{as}}}{(V/A)_{\mathrm{ms}}} \tag{4}$$

where $(V/A)_{\mathrm{as}}$ and $(V/A)_{\mathrm{ms}}$ denote the *V*/*A* ratio of mainshock and aftershock, respectively. The parameter κ was introduced to represent the relative intensity level of aftershock with respect to the mainshock.

6.2 Effect of parameter κ on the structural story damage demands

As mentioned above, it is insufficient to solely take the PGA as the relative intensity indictors to assess the effect of aftershocks on structures and the frequency characteristics of seismic sequence have a significant influence on engineering structures. Therefore, relative intensity index, κ, which considers the frequency characteristics of mainshock and aftershock, is proposed as evaluation criteria (i.e., Eq. (4)). For considering different values of parameter κ, the near-fault pulse-like records listed in Table 3 are divided into four groups according to the *V*/*A* ratio values. The *V*/*A* ratio intervals of these four groups are 0.13–0.17 s, 0.19–0.22 s, 0.23–0.27 s and 0.28–0.31 s, respectively. For each group, the average values of parameter κ are used in following analyses.

Firstly, the effect of relative intensity index κ on the structural story damage demands is discussed under a certain DI_o when subjected to the NP–NP seismic sequences. Figure 8 shows the effect of the parameter κ values on the structural story damage demands for DI_o of 0.4. It should be noted that the selected aftershock records in Fig. 8a–d are the consistent, while the values of parameter κ are different. This is because that *V*/*A* ratio of the selected mainshock records is different (i.e., see in Table 3). In Fig. 8, the structural story damage demands increase with the increase in parameter κ, and it increases more obviously on the ground floor. Moreover, we can make the same conclusion; when

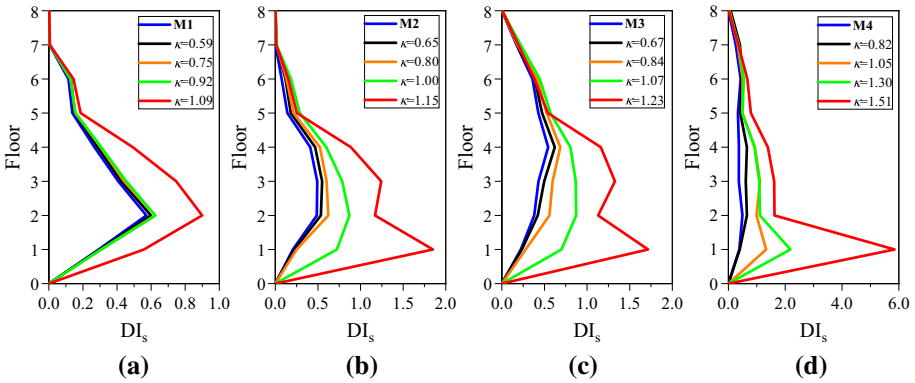

Fig. 8 Height-wise distribution of average story damage index computed from different relative intensity index κ values. **a M1** mainshock, **b M2** mainshock, **c M3** mainshock, **d M4** mainshock

the parameter κ is greater than 1.0, the story damage demands grow dramatically. On the contrary, the structural response is not obvious while the parameter κ is less than 1.0. This also proves that the stronger aftershock intensity (i.e., larger *V*/*A*) relative to the mainshocks could obviously increase the structural damage demands.

In order to further study the effect of aftershocks on different initial damage (i.e., $DI_o = 0.2$, 0.4, 0.6 and 0.8) structures, incremental story damage index (i.e., story damage increment caused by aftershock) is selected as the evaluation criteria. Figures 9 and 10 show the incremental story damage demands of the RC frame structure with different DI_o and κ values. It is evident that incremental story damage demands approximately increase with the increase in DI_o regardless of the values of κ. And this trend is mainly reflected in the bottom part of the structure. This explains that the collapse of structure usually occurs on the bottom story. In addition, under same of DI_o, the maximum incremental story damage demands increase with the values of κ. This situation further verifies that large *V*/*A* ratio of aftershocks relative to the mainshock will cause more serious damage.

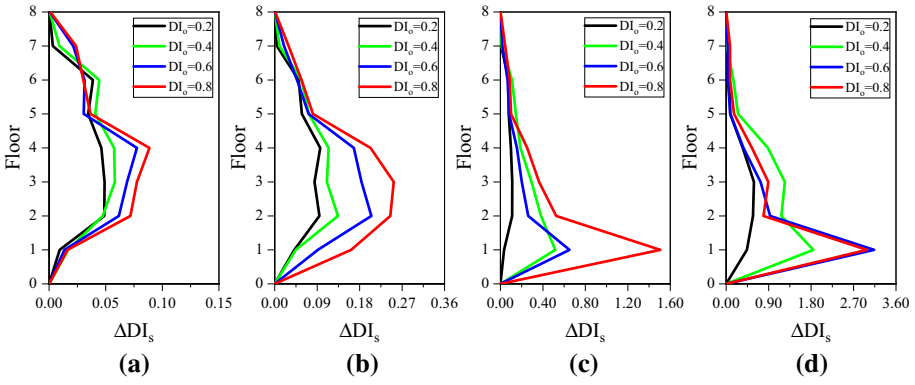

Fig. 9 The incremental story damage demands analysis of the **M2** mainshock under different relative intensity index values. **a** $\kappa = 0.65$, **b** $\kappa = 0.80$, **c** $\kappa = 1.00$, **d** $\kappa = 1.15$

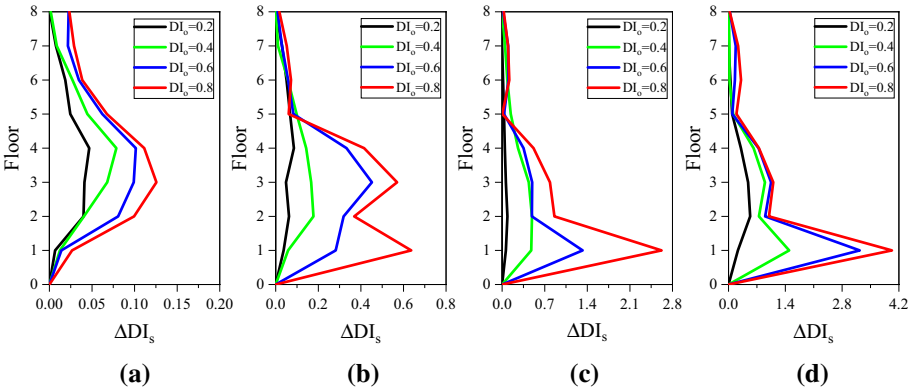

Fig. 10 The incremental story damage demands analysis of the **M3** mainshock under different relative intensity index values. **a** $\kappa = 0.67$, **b** $\kappa = 0.84$, **c** $\kappa = 1.07$, **d** $\kappa = 1.23$

6.3 Effect of parameter κ on the aftershock damage IDA curves

In this section, effect of parameter κ on the aftershock damage IDA curves in terms of aftershock collapse capacity is investigated under different mainshocks with a certain DI_o. For this purpose, the aftershock IDA of damaged building structure after mainshock action is performed. Figure 11 shows the aftershock IDA curves of different mainshocks when the DI_o is equal to 0.4. It should be noted that the parameter κ values of these figures are the same as those shown in the previous section. As can be seen from the four figures, with the increase in aftershock intensity (i.e., PGA_{as}), the aftershock damage IDA curve grows exponentially, and as the parameter κ value increases, the aftershock collapse capacity (i.e., $PGA_{c,\,as}$) decreases. In addition, in the case of low aftershock intensity (i.e., $PGA_{as} \leq 0.1$ g), the structural global damage index had no significant increase under the action of aftershock records. Therefore, the effect of smaller aftershocks on structures can be neglected. Otherwise, it also can be found that the *V/A* ratio value of mainshock is greater and the intensity of mainshock (i.e., PGA_{ms}) which makes structure reach the same initial damage state is smaller.

6.4 Effect of parameter κ on the normalized hysteretic energy

In this section, the damage demands of building model are investigated using the relative normalized hysteretic energy ΔNHE index which is defined as:

$$\Delta\mathrm{NHE} = \frac{\sum_{i=1}^{n} \Delta\mathrm{NHE}_{\mathrm{as}}}{\sum_{i=1}^{n} \mathrm{NHE}_{\mathrm{ms}}} \tag{5}$$

where $\Sigma\mathrm{NHE}_{\mathrm{ms}}$ is the sum of the normalized hysteretic energy of all building's members induced by single mainshock action and $\Sigma\Delta\mathrm{NHE}_{\mathrm{as}}$ is the sum of the normalized hysteretic energy induced by the aftershock of artificial seismic sequences, where the NHE is defined

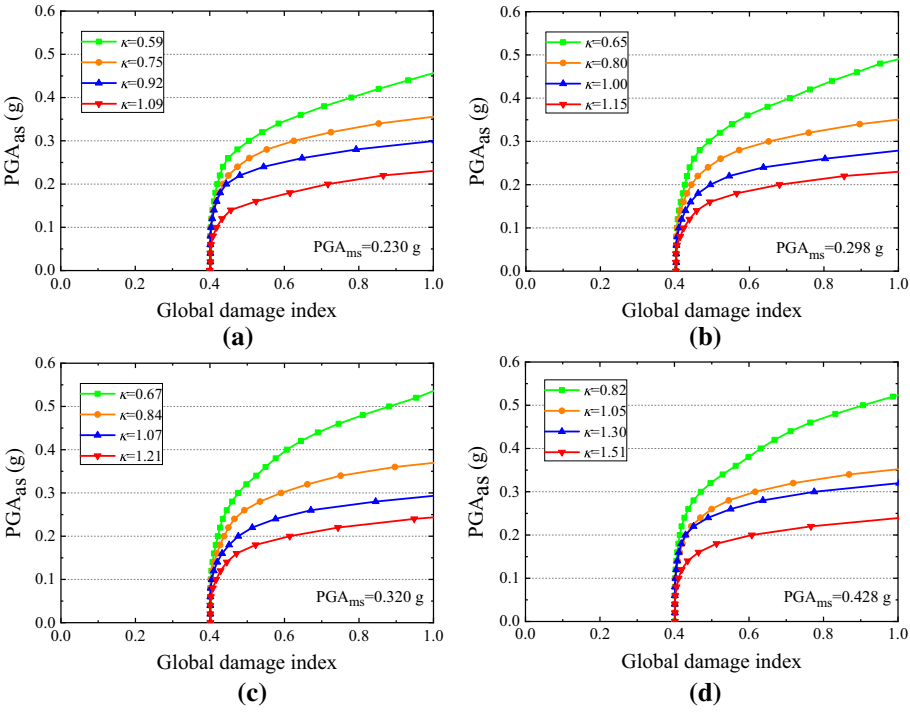

Fig. 11 Comparison of postmainshock aftershock IDA curves of different mainshocks when $DI_o = 0.4$. **a M1** mainshock, **b M2** mainshock, **c M3** mainshock, **d M4** mainshock

as $NHE = E_H/M_y\theta_u$, n is the total number of all structural members and E_H is the hysteric energy dissipation of member under ground motion.

Figure 12 illustrates the results of relative normalized hysteretic energy of frame model under NP–NP mainshock–aftershock seismic sequences with $DI_o = 0.4$. Obviously, seismic sequences strongly affect relative normalized hysteretic energy (i.e., ΔNHE) of building structure, in addition to the aforementioned damage indices. Furthermore, additional hysteretic energy highly depends on the ground motion characteristics of the aftershock. It is interesting to observe that when the parameter κ is greater than or equal to 1.0, the ΔNHE is obviously greater than that of the case with parameter $\kappa < 1.0$. This is also the reason why strong aftershocks (i.e., *V*/*A* of aftershock is greater than or equal to mainshock) lead to greater damage to buildings damaged by mainshock.

7 Conclusions

This study presented the damage demands assessment for the RC frame structure subjected to near-fault constructed mainshock–aftershock seismic sequences. The main innovation of this work is the quantification of the effects of aftershocks directly into the damage demands under different initial damage states. This study focused on investigating whether aftershock could increase collapse capacity and the story damage demands for the frame model with a different initial damage DI_o. For considering

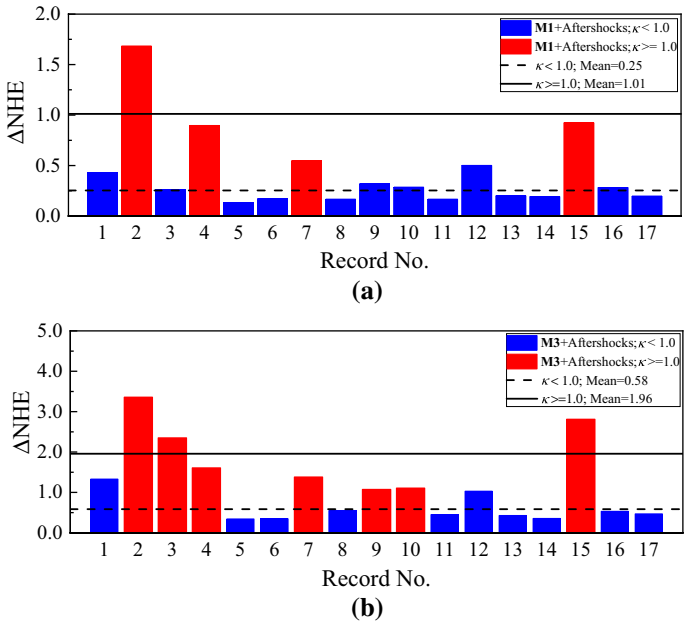

Fig. 12 Relative normalized hysteretic energy under different mainshocks with $DI_o = 0.4$. **a M1** mainshock, **b M3** mainshock

different frequency characteristics of seismic sequences, two sets of constructed mainshock–aftershock sequences were generated using a randomized approach. The following conclusions are drawn from this investigation:

- The collapse capacity of the RC frame structure decrease under mainshock–aftershock seismic sequences compared with single mainshock records regardless of the structural initial damage states. Furthermore, the aftershock collapse capacity depends on initial damage states of postmainshock-damaged structure, which decreases with the increase in DI_o.
- Near-fault pulse-like aftershocks induce larger story damage demands compared with ordinary aftershock ground motions which tends to concentrate in the ground story since it was anticipated that the frames could develop a ground soft story mechanism.
- The story damage demands in the RC frame structure tend to increase as the *V/A* ratio of the aftershock with respect to the mainshock relative intensity index, κ, increases. Particularly, this trend is more obvious when the κ value is greater than or equal to 1.0. Serious initial damage state has a significant effect on the incremental story damage demands.
- There is a general tendency that aftershock IDA curves decrease when the relative intensity of mainshock–aftershock seismic sequences increases. Similar conclusions are drawn about the aftershock collapse capacity.
- The relative hysteretic energy index highly depends on the ground motion characteristics of the aftershock. When the parameter κ is greater than or equal to 1.0, the effect of relative hysteretic energy index increases with the value of parameter κ.

Based on the results of this investigation, aftershocks have a significant effect on the postmainshock-damaged structures, especially when the intensity of aftershock is relatively large compared to the mainshock (i.e., $\kappa > 1.0$). Therefore, consideration should be given in the structural seismic design, such as increasing the ductility of the structure by increasing the reinforcement ratio. In addition, it can be found that structural collapse usually starts from the bottom of the structure, mainly due to shear failure. Therefore, the structural bottom story needs to be strengthened to improve the structural shear resistance.

Finally, it should be noted that more comprehensive research needs to be carried out. For example, more seismic sequences and the structures with different heights (i.e., different free-vibration characteristics) should be considered.

Acknowledgements The authors gratefully appreciate the supports by National Science & Technology Pillar Program during the Twelfth Five-year Plan Period of China under Grant No. 2014BAL05B03 and the National Natural Science Foundation of China under Grant No. 51378092 and 51578113.

Data availability The strong motion records used in this paper are obtained from the PEER Ground Motion Database. The website is http://ngawest2.berkeley.edu/, last accessed on December 2016.

References

Abdelnaby AE, Elnashai AS (2014) Performance of degrading reinforced concrete frame systems under the Tohoku and Christchurch earthquake sequences. J Earthq Eng 18:1009–1036. https://doi.org/10.1080/13632469.2014.923796

Amadio C, Fragiacomo M, Rajgelj S (2003) The effects of repeated earthquake ground motions on the non-linear response of SDOF systems. Earthq Eng Struct Dyn 32:291–308. https://doi.org/10.1002/eqe.225

Bertero VV, Wang TY, Popov EP (1974) Hysteretic behavior of reinforced concrete flexural members with special web reinforcement. Earthquake Engineering Research Center, University of California, Oakland

Cosenza E, Manfredi G (2000) Damage indices and damage measures. Prog Struct Eng and Mater 2(1):50–59

Durucan C, Durucan AR (2016) Ap/Vp specific inelastic displacement ratio for the seismic response estimation of SDOF structures subjected to sequential near fault pulse type ground motion records. Soil Dyn Earthq Eng 89:163–170. https://doi.org/10.1016/j.soildyn.2016.08.009

Faisal A, Majid TA, Hatzigeorgiou GD (2013) Investigation of story ductility demands of inelastic concrete frames subjected to repeated earthquakes. Soil Dyn Earthq Eng 44:42–53. https://doi.org/10.1016/j.soildyn.2012.08.012

Fragiacomo M, Amadio C, Macorini L (2004) Seismic response of steel frames under repeated earthquake ground motions. Eng Struct 26:2021–2035. https://doi.org/10.1016/j.engstruct.2004.08.005

Fragiadakis M, Papadrakakis M (2008) Modeling, analysis and reliability of seismically excited structures: computational issues. Int J Comput Methods 5(04):483–511

GB50010-2010 (2010) Code for design of concrete structures. Ministry of Housing and Urban–Rural Development of the People's Republic of China, Beijing, China. **(In Chinese)**

GB50011-2010 (2010) Code for seismic design of buildings. Ministry of Housing and Urban–Rural Development of the People's Republic of China, Beijing. **(In Chinese)**

Goda K (2012) Nonlinear response potential of mainshock—aftershock sequences from Japanese earthquakes. Bull Seismol Soc Am 102(5):2139–2156. https://doi.org/10.1785/0120110329

Goda K, Taylor CA (2012) Effects of aftershocks on peak ductility demand due to strong ground motion records from shallow crustal earthquakes. Earthq Eng Struct Dyn 41(15):2311–2330. https://doi.org/10.1002/eqe.2188

Hatzigeorgiou GD (2010a) Behavior factors for nonlinear structures subjected to multiple near-fault earthquakes. Comput Struct 88:309–321. https://doi.org/10.1016/j.compstruc.2009.11.006

Hatzigeorgiou GD (2010b) Ductility demand spectra for multiple near- and far-fault earthquakes. Soil Dyn Earthq Eng 30:170–183. https://doi.org/10.1016/j.soildyn.2009.10.003

Hatzigeorgiou GD, Beskos DE (2009) Inelastic displacement ratios for SDOF structures subjected to repeated earthquakes. Eng Struct 31:2744–2755. https://doi.org/10.1016/j.engstruct.2009.07.002
Hatzigeorgiou GD, Liolios AA (2010) Nonlinear behaviour of RC frames under repeated strong ground motions. Soil Dyn Earthq Eng 30:1010–1025. https://doi.org/10.1016/j.soildyn.2010.04.013
Hatzivassiliou M, Hatzigeorgiou GD (2015) Seismic sequence effects on three-dimensional reinforced concrete buildings. Soil Dyn Earthq Eng 72:77–88. https://doi.org/10.1016/j.soildyn.2015.02.005
Hosseinpour F, Abdelnaby AE (2017a) Effect of different aspects of multiple earthquakes on the nonlinear behavior of RC structures. Soil Dyn Earthq Eng 92:706–725. https://doi.org/10.1016/j.soildyn.2016.11.006
Hosseinpour F, Abdelnaby AE (2017b) Fragility curves for RC frames under multiple earthquakes. Soil Dyn Earthq Eng 98:222–234. https://doi.org/10.1016/j.soildyn.2017.04.013
Kalkan E, Kunnath SK (2006) Effects of fling step and forward-directivity on seismic response of buildings. Earthq Spectra 22(2):367–390. https://doi.org/10.1193/1.2192560
Kent DC, Park R (1971) Flexural members with confined concrete. J Struct Div ASCE 97(7):1969–1990
Kunnath SK, Reinhorn AM, Lobo R (1992) IDARC version 3.0: a program for the inelastic damage analysis of reinforced concrete structures. National Center for Earthquake Engineering Research Buffalo, NY
Malhotra PK (1999) Response of buildings to near-field pulse-like ground motions. Earthq Eng Struct Dyn 28(11):1309–1326
Mander JB, Priestley MJN, Park R (1988) Observed stress–strain behavior of confined concrete. J Struct Eng 114(8):1827–1849
Mazzoni S, Mckenna F, Michael H (2014) The OpenSees command language manual—version 2.4. Pacific Earthquake Engineering Research Centre Berkeley: University of California
Menegotto M, Pinto P (1973) Method of analysis for cyclically loaded reinforced concrete plane frames including changes in geometry and inelastic behavior of elements under combined normal force and bending. In: IABSE Symposium on resistance and ultimate deformability of structures acted on by well-defined repeated Loads, Lisbon
Morfidis K, Kostinakis K (2017) The role of masonry infills on the damage response of R/C buildings subjected to seismic sequences. Eng Struct 131:459–476
Moustafa A, Takewaki I (2011) Response of nonlinear single-degree-of-freedom structures to random acceleration sequences. Eng Struct 33:1251–1258. https://doi.org/10.1016/j.engstruct.2011.01.002
Park YJ (1984) Seismic damage analysis and damage-limiting design of R/C structures. Ph.D. thesis, Department of Civil Engineering, University of Illinois, Urbana, IL
Park YJ, Ang AHS, Wen YK (1985) Seismic damage analysis of reinforced concrete buildings. J Struct Eng 111(4):740–757
Rinaldin G, Amadio C, Fragiacomo M (2017) Effects of seismic sequences on structures with hysteretic or damped dissipative behaviour. Soil Dyn Earthq Eng 97:205–215. https://doi.org/10.1016/j.soildyn.2017.03.023
Ruiz-García J (2012) Mainshock–aftershock ground motion features and their influence in building's seismic response. J Earthq Eng 16:719–737. https://doi.org/10.1080/13632469.2012.663154
Ruiz-García J, Aguilar JD (2015) Aftershock seismic assessment taking into account postmainshock residual drifts. Earthq Eng Struct Dyn 44:1391–1407. https://doi.org/10.1002/eqe.2523
Ruiz-García J, Negrete-Manriquez JC (2011) Evaluation of drift demands in existing steel frames under as-recorded far-field and near-fault mainshock–aftershock seismic sequences. Eng Struct 33:621–634. https://doi.org/10.1016/j.engstruct.2010.11.021
Ruiz-García J, Marín MV, Terán-Gilmore A (2014) Effect of seismic sequences in reinforced concrete frame buildings located in soft-soil sites. Soil Dyn Earthq Eng 63:56–68. https://doi.org/10.1016/j.soildyn.2014.03.008
Tso WK, Zhu TJ, Heidebrecht AC (1992) Engineering implication of ground motion A/V ratio. Soil Dyn Earthq Eng 11(3):133–144
UBC (1997) Structural engineering design provisions. In: International conference of building officials (ICBO), vol 2. Whittier, CA
Vamvatsikos D, Cornell CA (2002) Incremental dynamic analysis. Earthq Eng Struct Dyn 31(3):491–514
Wang G, Wang Y, Lu W (2017) Damage demand assessment of mainshock-damaged concrete gravity dams subjected to aftershocks. Soil Dyn Earthq Eng 98:141–154
Zhai CH, Wen WP, Li S, Chen Z, Chang Z, Xie LL (2013) Damage spectra for the mainshock–aftershock sequence-type ground motions. Soil Dyn Earthq Eng 59:30–41. https://doi.org/10.1016/j.soildyn.2014.01.003
Zhai CH, Wen WP, Chen ZZ, Li S, Xie LL (2014) The damage investigation of inelastic SDOF structure under the mainshock–aftershock sequence-type ground motions. Earthq Eng Struct Dyn 45(2):1–12

Zhai CH, Wen WP, Li S, Xie LL (2015) The ductility-based strength reduction factor for the mainshock–aftershock sequence-type ground motions. Bull Earthq Eng 13:2893–2914. https://doi.org/10.1007/s10518-015-9744-z

Zhang YQ, Chen J, Sun CX (2017) Damage-based strength reduction factor for nonlinear structures subjected to sequence-type ground motions. Soil Dyn Earthq Eng 92:298–311. https://doi.org/10.1016/j.soildyn.2016.10.002